OBSERVATIONS BY SATELLITE ALTIMETRY OF SHORT SURFACE WAVE ENERGY IN THE DECEMBER 2004 SUMATRA TSUNAMI

Jim Gower

Institute of Ocean Sciences, Fisheries and Oceans Canada, Sidney, BC, V8L 4B2, Canada

ABSTRACT The main tsunami wave triggered by the December 2004 Sumatra tsunami was detected in the ocean south of India by satellite altimeters on Jason, Topex/Poseidon and Envisat. All three altimeters also detected shorter-wavelength (10 to 100 km), slower-propagating surface waves, spreading from the site of the earthquake. The shorter waves give additional information about the tsunami event, and can be used to better define the generating region in this, and future tsunamis. The properties of the area of shorter tsunami-generated waves may also be important in designing a future satellite-based detection system.

KEY WORDS: Tsunami, Altimetry, Surface waves, Dispersion

1. INTRODUCTION

The 26 December 2004 earthquake was the largest since satellite altimetry started in the 1970s, and gave peak-to-trough tsunami waveheights in mid-ocean of over a metre (Gower, 2005; 2006; NOAA, 2005). The Sumatra tsunami was detected by three of the four altimeters presently in orbit and giving sea surface height information. Each detected the spreading wave-front as it moved southwestwards into the Indian Ocean at about 750 km/hour (shallow water wave speed in 4500 m water depth), causing an initial rise in sea level. In addition, the altimeters also detected the disturbed region closer to the epicentre that expands with the slower velocities of higher frequency waves. The distribution of this wave energy provides important additional information on tsunami source location.

2. SATELLITE ALTIMETER OBSERVATIONS OF THE TSUNAMI FRONT

Figure 1 shows the tracks of the three satellites that clearly detected the main tsunami wave, and circles of equal range from 3.4 N, 94.2 E at the times of detection of the front near latitude 5 S for Jason-1 and Topex/Poseidon and 17 S for Envisat. The circles would show the positions of the front at these three satellite detection times if the ocean were of uniform depth. The front at the time of detection by Jason-1 would have hit the coast of eastern Sri Lanka and would be at about latitude 16 N in the northern Bay of Bengal. By the later time of detection by Envisat, the front would have passed to the west of India and would have hit the shore at all points in the Bay of Bengal.

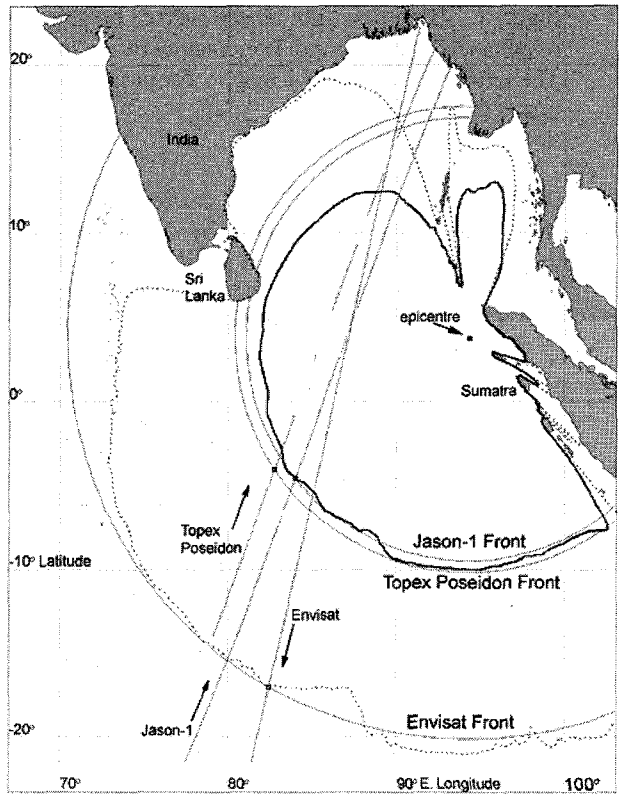

Figure 1. Tracks of Jason-1, Topex/Poseidon (ascending) and Envisat (descending) on which the tsunami was detected by satellite altimetry. Large circles are lines of equal range from the epicentre to satellite detection points (small squares at intersections of circles with the appropriate satellite tracks). The heavy solid and dotted lines are positions of tsunami fronts predicted using ETOPO5 bathymetry.

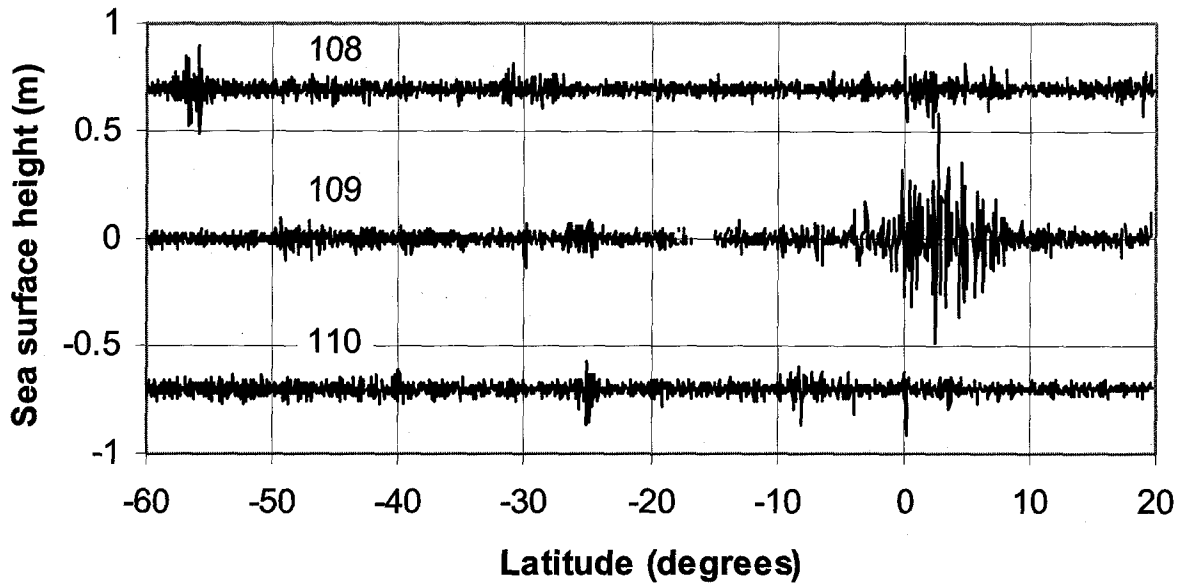

Figure 2. High-pass filtered sea surface heights from pass 129 of Jason-1 on cycles 108, 109 and 110. An area of enhanced wave energy is evident between latitudes 3 S and 8 N on the pass over the tsunami (129, cycle 109). The left-hand scale shows heights for pass 109. Data for passes 108 and 110 are displaced vertically by plus and minus 0.7 m

More accurate computations were carried out for the present study (Gower, 2006) by modeling the propagation of the tsunami as a shallow water wave travelling over bathymetry given by ETOPO5 (NOAA, 1988). This gives positions of the front at the heavy solid line for the Jason-1 detection time, and at the heavy dotted line for the Envisat detection time. The Jason-1 front is still roughly circular south of the equator, but shallower water in the Bay of Bengal slows the wave. such that Jason-1 and Topex/Poseidon should intercept the front a second time at about latitude 13 N. At the later time of the Envisat detection near 17 S, the front would have hit the coast of south-east India, but would still be at about 17 N in the northern Bay of Bengal where it would be detected again by the Envisat altimeter.

3. SATELLITE ALTIMETER OBSERVATIONS OF HIGHER FREQUENCY WAVES

In addition to detecting tsunami fronts, the Jason-1 altimeter also detected an area of greater height variability closer to the epicentre. High-pass filtered sea surface heights for this pass are shown in Figure 2. High variability is seen between 3 S and 8 N latitudes on cycle 109. The background level of variability can be assessed from the three similarly-filtered passes shown. These are all from pass 129, in cycles 108, 109 and 110.

The burst of high variability in cycle 109 in Figure 2 is interpreted as shorter waves generated in the same tsunami event as the longer waves, but propagating from the tsunami source region at lower velocities (E. Kulikov, pers. comm.). The altimeter height samples are consecutive one-second averages, each covering a distance of about 5 km along track. Data in Figure 2 were high pass filtered by subtracting smoothed heights (9-sample boxcar average), to pass wavelengths up to about 70 km. The minimum wavelength detectable is about 10 km (Nyquist limit), but aliased energy will be measured to the wavelength limit imposed by the instantaneous field of view of the altimeter, on the order of 5 km. The wavelength range is therefore 5 to 70 km, though at both wavelength extremes the cut-off will not be sharp.

The shorter-wave variability in Figure 2 peaks at a latitude of 2.9 N and drops to about half amplitude at latitudes of 0.4 S and 6.2 N. The Jason-1 track passes closest to the epicentre (Figure 1) at 6.0 N, at a distance of 765 km. At this point variability would be expected to be greatest, unless it can be argued that even the shortest waves detected would travel fast enough to have moved further from the epicentre, beyond the region sampled by Jason-1. The required velocity for this is about 400 km/hour. However, the shortest waves detectable by Jason-1 travel at about 320 km/hour in water 4000 m deep, so that these waves should still be present. In any case, a uniform distribution with azimuth would imply a symmetrical distribution of variability about the point of closest approach.

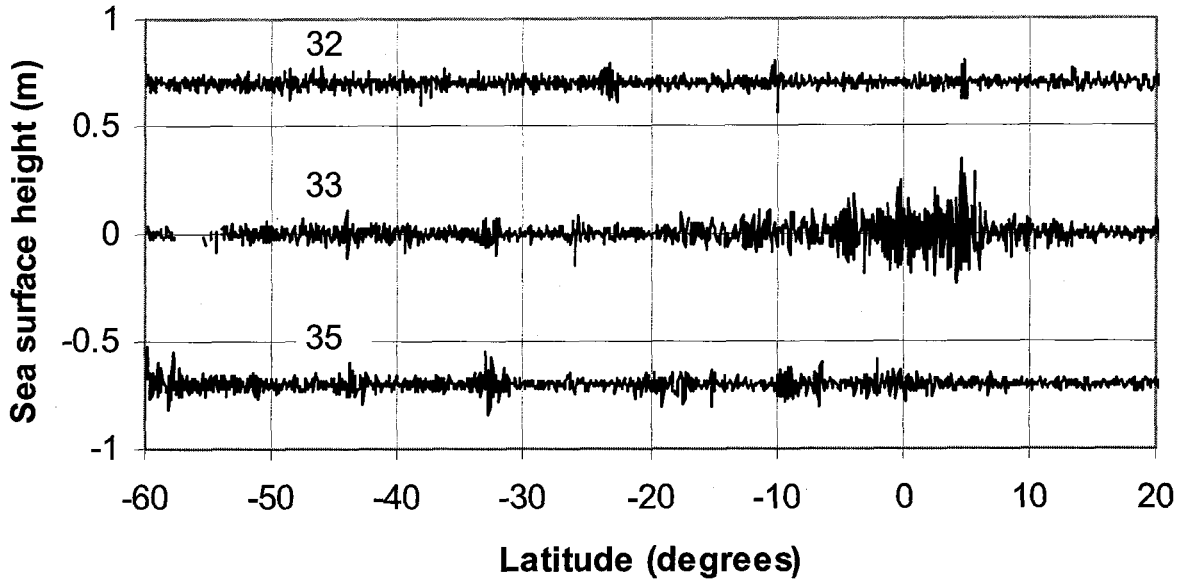

Figure 3. High-pass filtered sea surface heights from pass 352 of Envisat on cycles 32, 33 and 35. An area of enhanced wave energy is evident between latitudes 5 S and 7 N on the pass over the tsunami (352, cycle 33). Vertical scales as for Fig 2. Data for cycle 34 are not available.

The observed peak variability is significantly to the south of this point, indicating that these shorter waves are also focused to the southwest, as for the longest wavelengths.

When the data are filtered for a higher cut-off frequency, the wave energy distribution is shifted northwards. Filtering by subtracting heights smoothed with a 3-sample boxcar average, giving a band-pass of about 5 to 20 km, results in a distribution centred on 4.6 N and dropping to half amplitude at 3.0 and 7.7 N latitudes, with a drop in energy by about a factor 2. This filtering reduces the faster, longer-wave components which have propagated further to the south, and therefore shows variability closer to the latitude of closest approach.

The Topex/Poseidon and Envisat altimeters also detected regions of greater short-wave height variability. In the case of Topex/Poseidon, gaps in the data from latitude 1 S to 5 N prevent determination of the distribution of the waves, though an increase is observed between 6 N and 8 N where data exist. Envisat data (Figure 3) show the area of increased height variability, now reduced in amplitude to about 0.7 of Jason-1 and shifted to the latitude range 5 S to 6 N, compared to the total range 3 S to 8 N for Jason-1. This is roughly as expected, since the waves that defined the southern end of the latitude range will have propagated further south, while the northern end of the range is defined mostly by the azimuth distribution of wave energy.

Even shorter-wavelength surface wave energy, at wavelengths less than about 5 km, are detected by the altimeters as an increase in the Significant Wave Height (SWH), which is determined from the shape of the return signal. However, surface wind waves and swell tend to mask such an increase. The wave energy peak near latitude 5 N in Figure 2 would by itself correspond to an SWH of about one metre or less since the energy is observed to be decreasing at shorter wavelengths. It would therefore be masked by even a moderate surface wave field. Significant Wave Heights measured by Jason-1 are near 1.3 m on pass 129, cycle 109 in this area, and show no clear increase due to the tsunami. Measured values between 2.5 and 6 N latitude show both higher and lower values of SWH, with some unreasonably large, isolated, values over 5 m, which probably indicate tracking problems in this region of strong height variability. Most values of SWH in this latitude range are near 1.3 m.

4. CONCLUSIONS

The short wave energy provides an additional target for a satellite altimeter, providing confirmation of tsunami detection and localization of the tsunami source.

The observed distributions of short-wave tsunami wave energy in Figures 2 and 3 provides strong evidence against a significant tsunami source further north, such as proposed by Fine et al, (2005) and others. A source at 8 N, 94 E for example, would be closest to the Jason-1 path at about 10 N. Figures 2

and 3 show very little high frequency wave energy north of about 8 N, with distributions suggesting a source south of about 5 N.

Surface waveheight data from the altimeters, deduced from the shape of the backscattered radar pulse, could in principle be used to detect even shorter wave energy, but this is masked by wind-driven waves and swell.

Measurements of high-frequency wave energy in the tsunami using the hydrophone arrays installed by the Comprehensive Nuclear Test Ban Treaty Organization (www.ctbto.org) also show strong dispersion. Hanson and Bowman (2005) show spectrograms for the frequency range 5 to 25 mHz, corresponding to periods of 40 to 200 seconds, or wavelengths in mid ocean (4500 m depth) of 3 to 40 km, similar to the range in Figs 2 and 3. In a later paper (Hanson et al, in press) these data are used to localize the tsunami source region at these frequencies, confirming that energy arrives from the southern source only.

It has been noted that the Jason altimeter was in the right place at the right time to detect this tsunami. On the other hand, in a few hours a rapidly spreading tsunami presents an extensive target which has a good probability of intersecting the track of an altimeter in low, polar orbit. This tsunami was detected by three of the four altimeters presently in orbit.

Whether this detection rate is enough to make an altimeter-based tsunami monitoring system such as SOS (2005) a viable possibility, is still hard to determine. Alternatives, such as buoys and hydrophone arrays are also available. Buoy systems such as the US DART (Deep-ocean Assessment and Detection of Tsunamis, Gonzalez, 2005) have the advantages of placement (buoys can be positioned to provide warning to critical areas) and cost (on the order of $US100,000, compared to 100 to 1000 times higher for a satellite).

Buoys can also detect a much smaller tsunami signal. Gower and Gonzalez (2006) report detection of the Sumatra event by buoys in the Pacific at a level of a few millimeters. The bottom pressure recorders used by DART detect the time signature of tsunami waves, which is in a band (10 to 60 minute period) relatively free of confusing signals. A satellite altimeter detects the space signature of the waves in deep water. This is in a wavelength range (100 to 600 km) also occupied by mesoscale eddies, which provide a noise background of 5 to 30 cm rms, depending on position in the world's oceans (Nerem, 1994).

5. ACKNOWLEDGEMENTS

This work was supported by Fisheries and Oceans Canada and by the Canadian Space Agency (CSA) under the GRIP (Government Related Initiative Program). Data plotted here are those provided by the Radar Altimeter Database System (RADS) of the Technical University of Delft, Holland. The author is grateful to RADS data manager Eelco Doornbos and to colleagues Alexander Rabinovich and Isaac Fine for advice and useful discussions.

6. REFERENCES

Fine, I.B., A.B. Rabinovich and R.E. Thomson, 2005, The dual source region for the 2004 Sumatra tsunami, Geophysical Research Letters, 32, L16602, doi: 10.1029/2005GL023521.

Gonzalez, F.I., E.N. Bernard, C. Meinig, M. Eble, H.O. Mofjeld, and S. Stalin (2005): The NTHMP tsunameter network. Nat. Hazards, 35(1), Special Issue, U.S. National Tsunami Hazard Mitigation Program, 25–39.

Gower, J.F.R., 2005, Jason-1 detects the 26 December 2004 tsunami, Eos, 86, No. 4, 25 January, 2005, 37-38.

Gower, J.F.R, 2006, The 26 December 2004 tsunami measured by satellite altimetry, International Journal of Remote Sensing, in press

Gower, J. and F. Gonzalez, 2006, U.S. warning system detected the Sumatra tsunami, Eos, 87, No. 10, 7 March, 2006, 105, 108.

Hanson, J.A, and J.R. Bowman, 2005, Dispersive and reflected tsunami signals from the 2004 Indian Ocean tsunami observed on hydrophones and seismic stations, Geophysical Research Letters, 32, L17606, doi:10.1029/2005GL023783.

Hanson, J.A., Reasoner, C. and J. R. Bowman, 2006, High frequency tsunami signals of the great Indonesian earthquakes of 26 December 2004 and 28 March 2005, Bulletin of the Seismological Society of America, in press.

Nerem, R.S, E.J. Schrama, C.J. Koblinsky, B.D. Beckley, A preliminary evaluation of ocean topography from the TOPEX/POSEIDON mission, Journal of Geophysical Research, 99, 24565 (1994).

NOAA, 1988, Data Announcement 88-MGG-02, Digital relief of the Surface of the Earth, National Geophysical Data Center, Boulder, Colorado, 1988

NOAA, 2005, NOAA scientists able to measure tsunami height from space, http://www.noaanews.noaa.gov/stories2005/s2365.htm

SOS, 2005, http://www.satobsys.co.uk/GANDER/webpages/ganhome.html